Seasonal changes in canopy leaf area index and MODIS vegetation products for a boreal forest site in central Finland

Rautiainen, Miina

Finnish Environment Institute

2012

Rautiainen, M, Heiskanen, J & Korhonen, L 2012, 'Seasonal changes in canopy leaf area index and MODIS vegetation products for a boreal forest site in central Finland', Boreal Environment Research, vol. 17, pp. 72–84.

http://hdl.handle.net/10138/165139

other
publishedVersion

BOREAL ENVIRONMENT RESEARCH 17: 72–84
ISSN 1239-6095 (print) ISSN 1797-2469 (online) Helsinki 28 February 2012

Seasonal changes in canopy leaf area index and MODIS vegetation products for a boreal forest site in central Finland

Miina Rautiainen[1,*], Janne Heiskanen[1] and Lauri Korhonen[2]

[1)] *Department of Forest Sciences, P.O. Box 27, FI-00014 University of Helsinki, Finland (corresponding author's e-mail: miina.rautiainen@helsinki.fi)*
[2)] *School of Forest Sciences, P.O. Box 111, University of Eastern Finland, FI-80101 Joensuu, Finland*

Received 1 Dec. 2010, final version received 26 May 2011, accepted 26 May 2011

Rautiainen, M., Heiskanen, J. & Korhonen, L. 2012: Seasonal changes in canopy leaf area index and MODIS vegetation products for a boreal forest site in central Finland. *Boreal Env. Res.* 17: 72–84.

Seasonal change in leaf area index (LAI) is highly important in remote sensing of land surface phenology because LAI is a main driving factor of forest reflectance. We present a time series of *in situ* measurements of boreal forest LAI expanding throughout the growing period from budburst to senescence. We measured the LAI of 20 stands at approximately two-week intervals between mid-May and mid-September in 2009 in southern Finland using hemispherical photography. We compared our field reference data with landscape-level MODIS surface reflectance trajectories, vegetation indices and LAI products. Our results showed that the timing of maximum LAI varies in different forest types. In general, the MODIS-based vegetation indices followed the general trend of spring–summer canopy LAI well. The MODIS LAI product, on the other hand, portrayed well the spring build-up of canopy-level foliage of broadleaved stands but began to decrease earlier in the fall than the ground reference LAI.

Introduction

Land surface phenology is defined as the seasonal variation in vegetated land surfaces observed by remote sensing instruments (Friedl *et al*. 2006, Morisette *et al*. 2009). To be able to detect phenological phases from remote sensing data sets, phenological variation must be characterized by changes in the optical properties of vegetation elements or by changes in structural properties of canopies (e.g., increase in leaf area or canopy closure) that are measurable in the spatial and spectral resolution of satellite images (e.g., Kobayashi *et al*. 2007, Rautiainen *et al*. 2009). Only medium to coarse resolution satellite images can provide phenological monitoring with global coverage and regularly repeated observations (Cleland *et al*. 2007, White *et al*. 2009). Therefore, many traditional phenological variables, such as budburst, flowering, or ripening of berries and fruits, that have only a small effect on canopy reflectance, cannot be readily interpreted from optical satellite images.

Seasonal change in green biomass or leaf area index (LAI) is highly important in remote sensing of land surface phenology because LAI is the main driving factor of forest reflectance recorded by space-borne satellite sensors. Hence, LAI offers a quantitative measure with a physical interpretation for monitoring phenological phases from satellite images. LAI is also measurable in the field. A recent intercomparison

Editor in charge of this article: Jaana Bäck

showed that a general problem in the validation of global-scale LAI products is the lack of ground reference data on the seasonal variability of different land surface types (Garrigues *et al*. 2008), because LAI measurements are typically carried out at the peak of the growing season (e.g. Morisette *et al*. 2006). Furthermore, information on both the temporal build-up and senescence of foliage are needed for various climate and land surface modeling purposes.

Ganguly *et al*. (2010) identified high latitude ecosystems as a key biome requiring further investigations in the interpretation of satellite image based phenology metrics and development of operational land cover dynamics (phenology) products. The reasons for this are versatile: in the boreal region, the seasonal monitoring of vegetation using optical satellite images is hindered by a persistent cloud cover, low solar zenith angles as well as the complex structure of coniferous canopies that is difficult to take into account in remote sensing algorithms. Topical problems in remote sensing of seasonal vegetation dynamics of boreal forests are related to defining the onset and end of the growing season, upscaling ground measurements to sensor resolution in heterogeneous landscapes and eliminating the spectral noise resulting from the presence of late-spring snow.

Previously, seasonal changes in boreal forest LAI have been assessed in the BOREAS project where LAI was measured three times during the growing season in Canadian Jack pine and Black spruce forests (Chen 1996), and in the GEWEX experiment in eastern Siberia where LAI of larch forests was measured four times (Kobayashi *et al*. 2007). In this case study, we present seasonal *in situ* measurements of Finnish boreal forest LAI expanding throughout the whole growing period from budburst to early senescence at two-week intervals and representing typical species composition and a wide range of stand structures. We compare our field reference data with landscape-level MODIS surface reflectance trajectories, spectral vegetation indices and LAI products. In other words, we investigate whether changes in LAI based on field measurements are visible in concurrent coarse resolution satellite images, and if a landscape-level analysis of the phenological cycle of a boreal forest area is feasible based on such data sets. Finally, we briefly discuss potential sources of error in predicting the timing of phenological phases of a boreal forest area using coarse resolution satellite data and hemispherical images.

Material and methods

Study site

Our study site, Hyytiälä, is located in southern Finland (61°50´N, 24°17´E) and belongs to the southern boreal zone. The annual mean temperature is 3 °C and precipitation is 700 mm. Dominant tree species are Norway spruce (*Picea abies*), Scots pine (*Pinus sylvestris*) and birches (*Betula pubescens*, *Betula pendula*). Understory vegetation at the study site is composed of two layers: an upper understory layer (low dwarf shrubs, graminoids, herbaceous species) and a ground layer (mosses, lichens).

The growing season typically begins in early May and senescence occurs in late September. According to the traditional phenological observations (www.metla.fi/metinfo/fenologia/index-en.htm), in 2009 in the region around our study site, the first birch leaves emerged on 13–17 May, reached their maximum size on 10–16 June and turned yellow between 26 September and 3 October. The height growth of Scots pine, on the other hand, began on 8–15 May and was completed by 10–17 July.

In 2009, we selected 20 stands from the Hyytiälä forest area (7 × 7 km) for seasonal LAI measurements (Table 1). The stands represented different age classes (stand age: 25–100 years) and species compositions (Norway spruce, Scots pine, silver and downy birches) that are typical to the southern boreal forest zone. A regular stand inventory was carried out in all the plots to provide background information on the stand structure.

LAI measurements

We estimated LAI, the hemisurface green leaf area per unit area of ground, using hemispherical photography at approximately two-week intervals starting from mid-May (day of year, DOY

134) and ending in mid-September (DOY 254). Hemispherical images were obtained during standard overcast sky conditions at any time of the day or during clear sky conditions in early morning or late evening (i.e. when the solar elevation angle was smaller than 16°).

We took hemispherical images at twelve points in each stand and applied the sampling scheme recommended by the VALERI (Validation of Land European Remote Sensing Instruments, URL: http://www.avignon.inra.fr/valeri) network: a cross with measurement points placed at 4-m intervals on a south–north transect (6 points) and on a west–east transect (6 points). The measurement points were permanently marked with wooden sticks, i.e. the hemispherical images were acquired from the exact same locations throughout the growing season.

The camera used to take the hemispherical images was a Nikon Coolpix 8800 equipped with a FC-E9 fisheye converter. The camera was mounted on a tripod and rotated so that its base was always directed towards the north. The camera was leveled using a bubble level placed on the lens cover. Measurement height (distance from the ground to the lens) was approximately 1.3 m in forests and 0.5 m in seedling stands. Images were stored in an uncompressed raw image format at the resolution of the CCD sensor (3280 × 2454 pixels). No corrections for possible projection errors of the fisheye converter were applied, i.e. the projection was assumed to be equidistant. We set the aperture of the camera manually while exposure time was determined automatically. The exposure was decreased by one stop to account for the camera's tendency to overexposure in dense forests (i.e., forests with a high LAI) (Zhang *et al*. 2005). The exposure time ranged from 1/20 seconds to 8 seconds, depending on the light conditions and the time of the day.

The image data were analyzed using scripts implemented by us in the MATLAB® programming environment (MathWorks Inc. 2010). The hemispherical images were thresholded using an edge-detection based algorithm developed by Nobis and Hunziker (2005). This algorithm selects the threshold that maximizes the brightness difference between the pixels on the crown and sky sides of the edges, and therefore pro-

Table 1. Stand variables of the study stands in Hyytiälä.

Stand ID	Dominant species	Mean tree height (m)	Basal area (m^2 ha^{-1})	Site type
Broadleaved stands				
E1	Birch	19.1	11	mesic
F1	Birch	13.8	14	mesic
U16	Birch	14.0	21	mesic
U17	Birch	11.7	27	herb-rich
H5	Birch	14.1	21	herb-rich
H3	Birch	14.9	11	herb-rich
Coniferous stands				
A1	Scots pine	17.5	25	herb-rich
A5	Scots pine	18.6	24	mesic
D3	Scots pine	17.8	21	sub-xeric
E7	Norway spruce	13.3	32	mesic
U26	Norway spruce	16.8	25	mesic
U27	Norway spruce	15.2	21	mesic
Mixed stands				
D4	Norway spruce	16.5	28	mesic
E6	Norway spruce	10.2	22	mesic
E5	Birch	23.1	27	mesic
I2	Birch	11.9	20	herb-rich
U19	Scots pine	22.9	42	mesic
U18	Scots pine	16.5	26	sub-xeric
Seedling stands				
G1	Birch	2.2	1	mesic
I4	Birch	2.4	4	mesic

duces consistently similar gap fractions even in different light conditions. However, as one threshold value was used for the entire image, the background sky had to be evenly lit to ensure good performance of the algorithm. After the thresholding, the gap fractions were calculated for concentric rings 0–15°, …, 45–60° as the proportion of sky (white) pixels within each ring.

Finally, LAI was computed from the gap fractions for a solid angle extending 60° from zenith using the standard method behind the LAI-2000 Plant Canopy Analyzer (LAI-2000 PCA, Welles and Norman 1991) limited to the uppermost four rings (Li-Cor Inc., Nebraska, USA). We noticed that a smoother time series of LAI was obtained by limiting the analyzed section of the hemispherical images to ±60° from nadir instead of applying ±75° from nadir as done by the commonly used LAI-2000 PCA instrument (LI-COR, Inc.). An explanation for this could be the use of a single threshold value for the entire image. When the entire image area is evaluated by the thresholding algorithm, the final threshold is an average, and the gap fractions may be biased near the zenith (brightest background) and near the horizon (dim background). The effect of the first ring (0°–15°) on the final LAI is small, but errors in the fifth ring (60°–75°) gap fraction have a considerable influence.

Each image was checked for possible problems (e.g. fuzziness, uneven cloud cover) in order to ensure a good discrimination between the sky and tree crowns while preserving the fine structure of the canopy. A few images were excluded from the analyses due to low quality.

We abbreviate effective canopy LAI obtained through this process as LAI_{eff}. It is called an effective leaf area index (and not a 'true' leaf area index) because it does not account for the clumping of foliage.

Satellite data

In the remote sensing part of the study, our aim was to investigate whether changes in LAI based on field measurements are visible in concurrent coarse resolution satellite images. We examined mean values and standard deviations of three Moderate Resolution Imaging Spectroradiometer (MODIS, Collection 5) data products for our study area: surface reflectances, vegetation indices (Table 2) and LAI. The data enabled a landscape-level analysis (7 × 7 km) of the phenological cycle of a boreal forest area.

First, we examined a time series of MODIS surface reflectance products (MOD09A1, 8-Day composite) which provide estimates of the surface spectral reflectances for each reflective MODIS band as it would have been measured at ground level without atmospheric scattering or absorption (i.e. reflectances are corrected for the effects of atmospheric gases and aerosols) (Vermote *et al*. 1997). The product contains the best possible observation for an 8-day period based on high observation coverage, low view angle, absence of clouds or cloud shadow, and aerosol loading. The spatial resolution of the data is 500 m. Next, we looked at the MODIS vegetation indices (MOD13Q1, 16-day composite) that include the normalized difference vegetation index (NDVI, based on red and NIR bands) and the enhanced vegetation index (EVI, based on red, NIR and blue bands), and have a spatial resolution of 250-m (Huete *et al*. 2002). In addition, we examined the reduced simple ratio (RSR, based on the red, NIR and SWIR MODIS surface reflectances) using similar SWIR band minimum and maximum values for the entire growing period. The equations of the vegetation indices are provided in Table 2. Finally, we evaluated against our *in situ* data the MODIS LAI product

Table 2. Spectral vegetation indices (SVI's) applied in this study. [BLUE = surface reflectance factor for MODIS band 459–479 nm; RED = surface reflectance factor for MODIS band 620–670 nm; NIR = surface reflectance factor for MODIS band 841–876 nm, and SWIR= surface reflectance factor for MODIS band 1628–1652 nm.]

Vegetation index	Abbreviation and equation
Normalized difference vegetation index	NDVI = (NIR – RED)/(NIR + RED)
Enhanced vegetation index	EVI = 2.5[(NIR – RED)/(NIR + 6RED – 7.5BLUE + 1)]
Reduced simple ratio	RSR = (NIR/RED)[($SWIR_{max}$ – SWIR)/($SWIR_{max}$ – $SWIR_{min}$)]

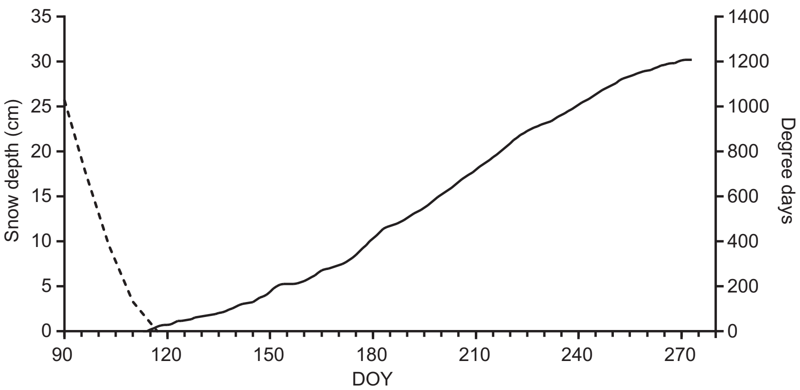

Fig. 1. Degree days (solid line) and snow depth in forest (dashed line) at the Hyytiälä study site as a function of day of year (DOY) in 2009. Measurements were made at the SMEAR flux tower in the center of the study area.

(MOD15A2, 8-day composite) which is retrieved from atmospherically corrected bidirectional reflectance factors in the red and NIR channels using a radiative transfer model for vegetation media (Knyazikhin *et al*. 1998, Yang *et al*. 2006). The spatial resolution of the data is 1 km.

We screened the quality flags of the products and used only values classified as "best possible results" for land pixels, e.g. for the LAI product we used only main algorithm retrievals without cloud contamination. This reduced the number of observations in the time series but guaranteed better quality data. Another challenge was that direct comparison of *in situ* LAI_{eff} measurements and MODIS data is not possible due to the large difference in spatial scale. Therefore, we upscaled our *in situ* LAI measurements to a landscape-level LAI estimate using the Finnish CORINE Land Cover 2006 database (CLC2006, 2006). According to the land cover data, our study area is composed of the following forest classes: 2.1% broadleaved forests, 58.4% coniferous forests, 16.6% mixed forests and 22.9% open areas, seedling stands and clear cuts. First, we classified our stands into groups which correspond to the CORINE Land Cover groups (i.e. six broadleaved, six coniferous, six mixed and two seedling stands shown in Table 1). Next, we computed average LAI_{eff} time series for each group. Finally, we calculated a mean landscape-level LAI_{eff} from the averaged *in situ* measurements by weighting each of the time series representing the four forest classes according to their coverage in our 7 × 7-km study area. According to the MODIS land cover classification scheme (Friedl *et al*. 2010) the study area is classified mostly as evergreen needleleaf forest (89% of study area).

Results and discussion

Snow melted in the Hyytiälä forests on approximately 25 April 2009 (DOY 115), and the thermal growing season (i.e. the date preceded by five consecutive days with daily mean temperature above +5 °C) began on 30 April (DOY 120) (Fig. 1). This was followed by a rapid unfolding and expansion of leaves which occurred between DOY 140 and 150 in broadleaved, mixed and seedling stands (Fig. 2). Throughout the field campaign, fluctuations of 10%–15% in LAI_{eff} were observed in the coniferous stands, especially in the densest stand (Fig. 2B, LAI_{eff} > 3.5). Differences were observed in the timing of maximum LAI_{eff} in the different forest types: in broadleaved and mixed stands maximal leaf area was reached by mid-July (DOY 194), whereas in coniferous and seedling stands foliage growth marginally continued until late August (DOY 238) (Fig. 3). However, one should note that the measurement height was lower in the seedling stands, and the LAI_{eff} estimate also includes understory vegetation growing between the seedlings.

The first measurements (DOY 134–139, Fig. 2) in the broadleaved (deciduous) stands correspond to woody area index (WAI) since no leaves had emerged yet. Thus, based on the measurements, we can estimate a midsummer mean WAI/LAI for the birch stands by taking the ratio of the first measurements and maximum

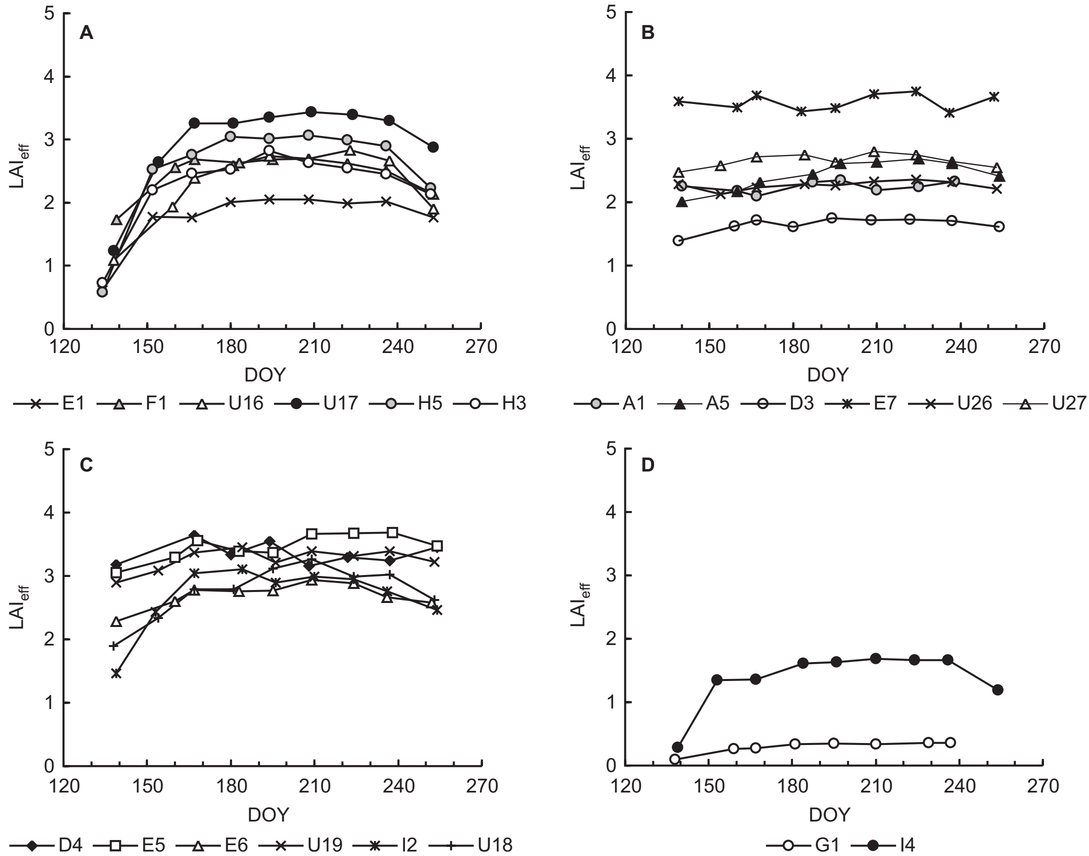

Fig. 2. The seasonal course of effective leaf area index (LAI_{eff}) measured in Hyytiälä in 2009 as a function of day of year (DOY). (**A**) six deciduous stands, (**B**) six coniferous stands, (**C**) six mixed coniferous-deciduous stands, and (**D**) two seedling stands. The symbols indicate different stands.

LAI_{eff} measurements for each stand. Computed this way, the mean WAI/LAI ratio for birch stands is 0.35 ± 0.16 SD. However, we did not apply this woody area correction to the LAI_{eff} estimates, since similar estimates of WAI were not available for the coniferous and mixed stands and because this correction method does not take into account (marginal) height growth of trees during the summer.

Using hemispherical digital photography to measure LAI contains inherently several problems, which have been reviewed by, for example, Jonckheere *et al*. (2004). Specific issues related to measuring a long time series of canopy LAI_{eff} using the hemispherical images include careful considerations of exposure, weather conditions and image processing methods. Therefore, ensuring consistent quality of an image acquisition and processing chain over a long period is challenging. The irregular fluctuations in our LAI_{eff} time series (Fig. 2) are likely due to measurement uncertainty since sudden changes in the canopy structure (e.g. annual needle cycle) are not expected to be very large. Another problem is separating the role of increase in woody and foliage materials in the hemispherical images: especially in young stands, tree height growth (which is a phenological phenomenon itself) may contribute to the decrease in canopy gap fractions (i.e. increase in LAI_{eff}) during the summer. Finally, changes in coniferous shoot structure (i.e. changes in needle-to-shoot area ratio, Chen 1996) during the summer may result in biased quantification of changes in canopy LAI.

According to ground-based observations of the national phenology network (www.metla.fi/

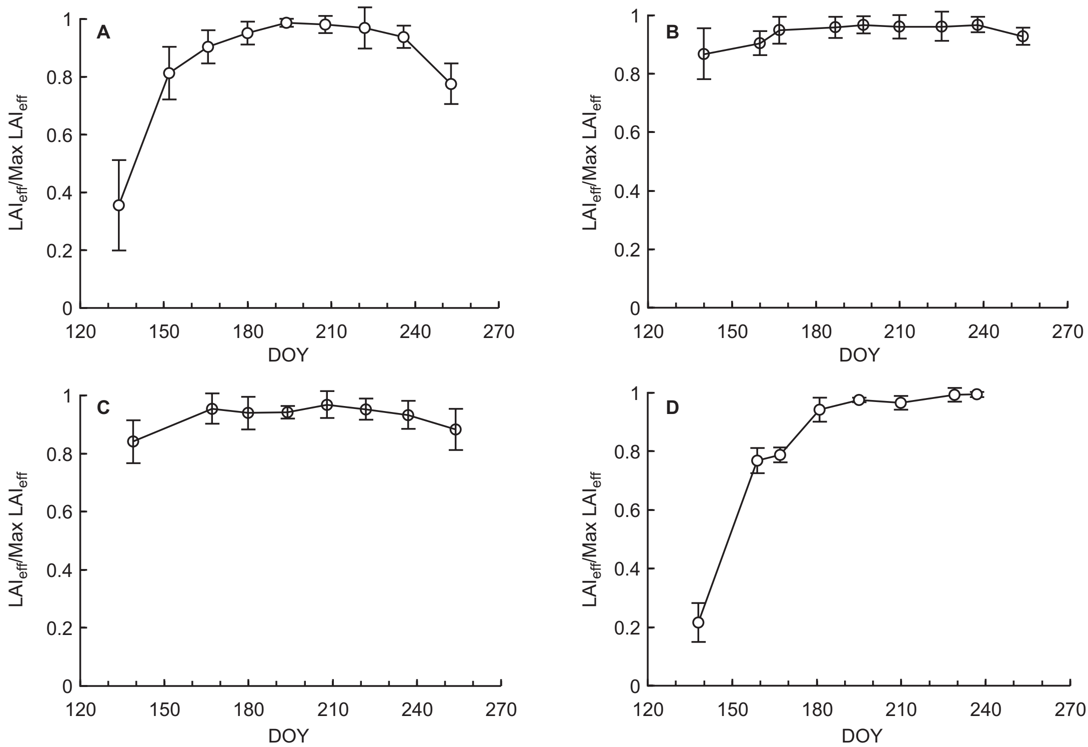

Fig. 3. The relative LAI_{eff} (i.e. LAI_{eff} at a given DOY divided by the seasonal maximum LAI_{eff}) obtained from *in situ* measurements. (**A**) deciduous stands, (**B**) coniferous stands, (**C**) mixed coniferous-deciduous stands, and (**D**) seedling stands. The error bars show standard deviations. Note that relative LAI_{eff} does not reach one in **A**–**C** because the curves show mean values for all stands. i.e. the maximal LAI_{eff} values were not reached on the same date in all the stands.

metinfo/fenologia/index-en.htm), in 2009 birches reached full leaf size already in mid-June and continued their height growth until August whereas our *in situ* LAI_{eff} (which may, on the other hand, also include contributions from height growth) continued to increase approximately from 5% to 8% from mid-June to mid-July (Fig. 3A). This may indicate problems for the use of traditional phenological observations as the validation data for seasonal detection algorithms in remote sensing. In other words, well-known phenological variables (e.g. emerging of leaves, flowering, ripening of berries) cannot be readily interpreted from satellite images since remote sensing is based on the interpretation of scattered electromagnetic radiation, and these variables are not the main driving factors of forest reflectance. Another problematic period is early senescence in late August and early September: indirect optical devices for measuring LAI_{eff} (such as the LAI-2000 PCA or hemispherical photography) do not detect the loss of green leaf area since the leaves are still attached to the trees even though they have begun to turn yellow. In this case, the use of phenological webcams (Richardson *et al*. 2007) or continuously monitoring PAR or transmittance sensors placed in the study area would provide valuable ancillary data for interpreting the LAI_{eff} time series and matching it with satellite reflectance data. Finally, this also raises a question concerning the applicability of LAI as a descriptor of the length of the growing season (or seasonal changes in primary productivity) in boreal forests. In deciduous and mixed forests, the beginning of the growing season can efficiently be determined through observations of LAI, but in pure coniferous forests, the seasonal course of LAI_{eff} is not dynamic enough to characterize the start of growing season in the spring. Therefore, other indicators, such as remotely sensed changes

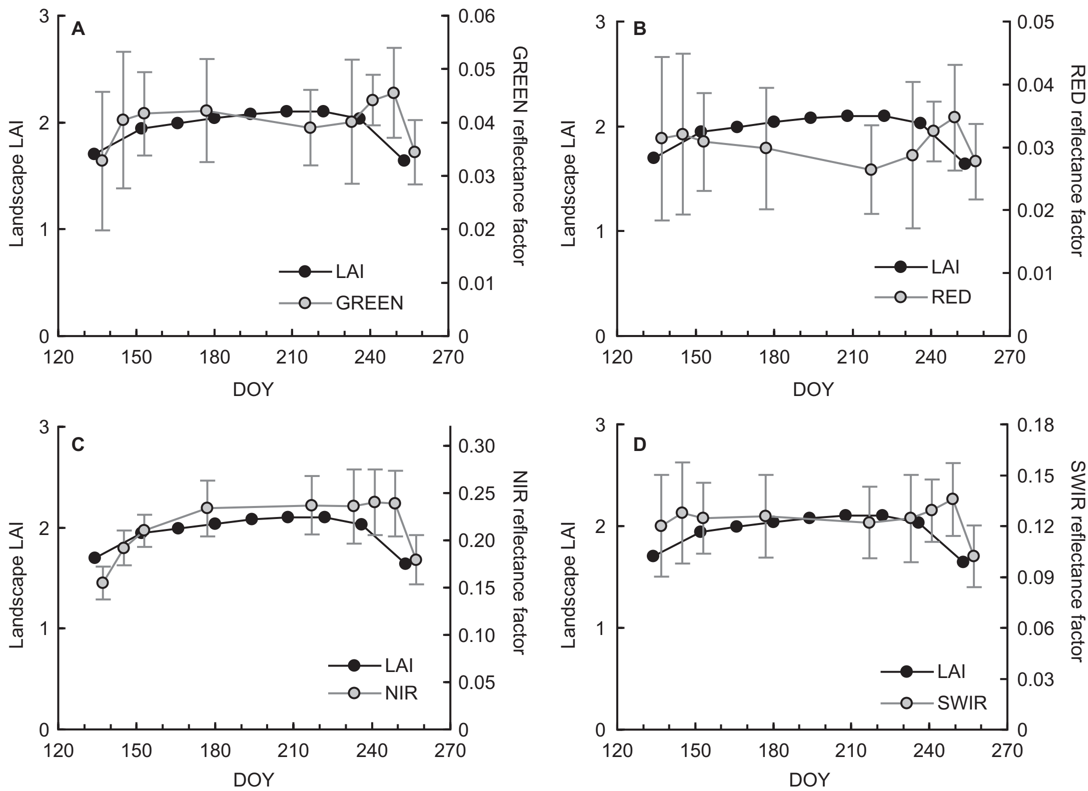

Fig. 4. Landscape-level LAI (7 × 7 km) upscaled from *in situ* measurements and MODIS surface reflectances as a function of day of year (DOY). (**A**) LAI and green reflectance (band 4, 545–565 nm), (**B**) LAI and red reflectance (band 1, 620–670 nm), (**C**) LAI and NIR reflectance (band 2, 841–876 nm), and (**D**) LAI and SWIR reflectance (band 6, 1628–1652 nm).

in the spectral properties of the vegetation, may have potential in determining growing season length (or seasonal changes in photosynthetic efficiency) also in coniferous forests.

As the first part of detecting seasonal changes in remote sensing data we compared landscape-level LAI_{eff} with MODIS surface reflectances (Fig. 4). Mean surface reflectances in the green (545–565 nm) and SWIR (1628–1652 nm) bands first increased as canopy LAI_{eff} increased during May, then dropped slightly during the stable phase of canopy LAI_{eff} in July (DOY 177–233) and finally increased in August when canopy LAI_{eff} began to gradually decrease. On the other hand, surface reflectances in the red band (620–670 nm) decreased as LAI_{eff} of the canopies increased, and vice versa. Both visible bands displayed a short peak in surface reflectances in early September (DOY 249). The results clearly indicate that LAI_{eff} is not the only factor determining the seasonal course of forest reflectance. For example, the peak-like changes in MODIS surface reflectances (with the exception of the NIR band) during early June and early September could possibly be linked to the rapid ongoing changes in either understory or leaf optical properties. However, the standard deviations of the surface reflectances are relatively large, hence making definite conclusions about the reflectance peaks is not possible. Finally, as already noted, the NIR band (841–876 nm) followed both the buildup and decline in canopy foliage relatively tightly. This is logical since NIR reflectance in boreal forests should be mainly driven by canopy structure (e.g., Rautiainen and Stenberg 2005).

Next, we looked at the seasonal trajectories of three spectral vegetation indices (Fig. 5). Previously, based on data obtained during 1986–2006, NDVI-defined trends for onset, end and length of the growing season were noted as reliable in

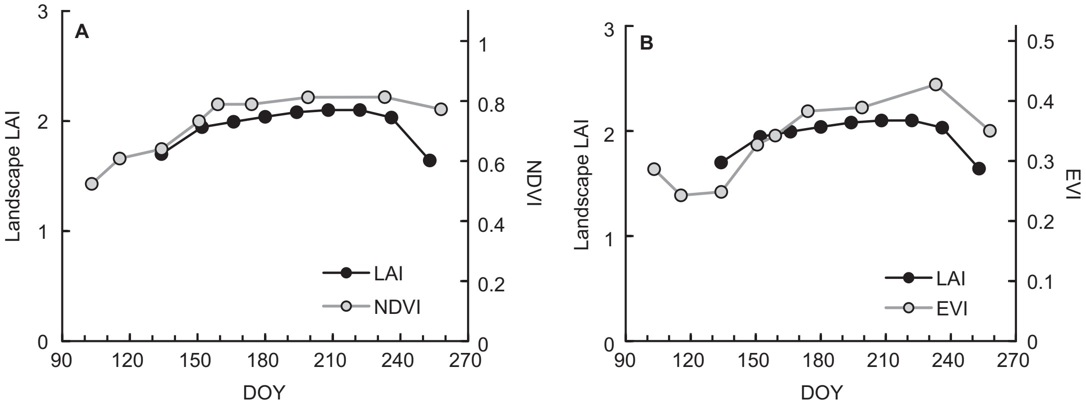

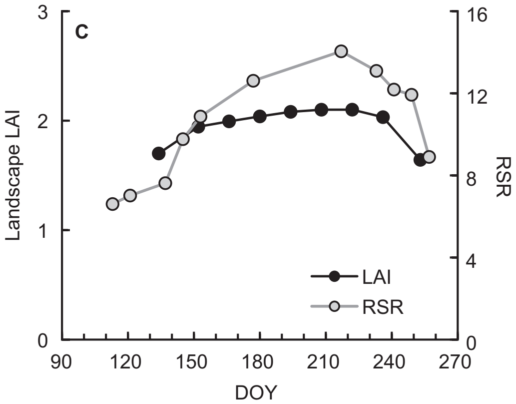

Fig. 5. Landscape-level LAI (7 × 7 km) up-scaled from *in situ* measurements and vegetation indices as a function of day of year (DOY). (**A**) LAI and NDVI (MOD13Q1), (**B**) LAI and EVI (MOD13Q1), (**C**) LAI and RSR (computed from MOD09A1).

the majority of Fennoscandia due to the high correlations in spring and rather low bias in fall (Karlsen *et al*. 2009). In our study area, NDVI captured the spring and summer development of canopy LAI_{eff} well. However, it did not react to the decrease in LAI in September and would thus have overestimated the length of the growing period. EVI, on the other hand, followed the general trend of LAI_{eff} well, but exhibited a small peak (unrelated to changes in canopy LAI_{eff}) during early senescence in mid-August. The poor performance of NDVI and EVI in detecting the fall transition may be due to the differences in the greening and yellowing cycle of the understory and overstory which also causes difficulties in applying simple vegetation index techniques to detect the start of season from satellite images (Doktor *et al*. 2009). The third vegetation index, RSR, captured the timing of both the spring and fall transitions well, but did not depict the stable LAI_{eff} phase during July. Even though none of the vegetation indices performed superiorly over the others in our single-year analysis, RSR followed the leaf build-up and senescence transitions of boreal forest canopy layers notably well. In the future, if landscape-level imaging spectroscopy data becomes routinely available, applying also narrow-band vegetation indices (e.g. the photochemical reflectance index (PRI); Garbulsky *et al*. 2011) may enable determining the length of the growing period in boreal forests more accurately.

Next, we compared our landscape-level LAI estimates with the MODIS LAI product (Fig. 6). The MODIS LAI portrayed well the spring time build-up of canopy-level foliage in broadleaved and seedling stands (Fig. 6A and D). However, the MODIS LAI values started to decrease a week earlier than field reference LAI. This may be either an artifact due to cloud contamination or temporal spacing of the measurements, or an actual observation due to some birch leaves turning yellow already in August even though the majority turned yellow during September. This would mean that the red surface reflectances used by the MODIS LAI retrieval algorithm started to increase but the leaves still contributed

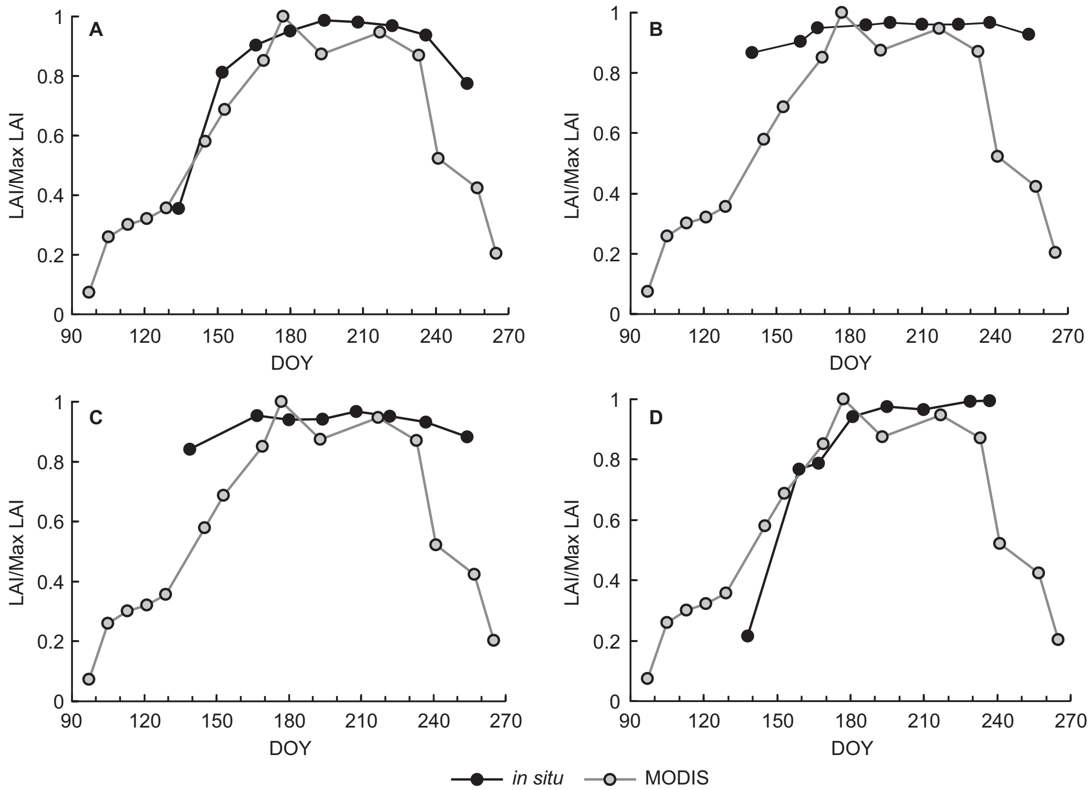

Fig. 6. Relative LAI_{eff} (i.e. LAI_{eff} at a given DOY divided by the seasonal maximum LAI_{eff}) obtained from *in situ* measurements and relative MODIS LAI (MOD15A2) (i.e. MODIS LAI on a given DOY divided by the seasonal maximum MODIS LAI). (**A**) deciduous stands, (**B**) coniferous stands, (**C**) mixed coniferous-deciduous stands, and (**D**) seedling stands.

to LAI measured by the hemispherical images though the optical transmittance properties of the leaves should have changed. (In future, it might be possible to validate this statement by separating yellow and red leaves from green leaves in hemispherical images using RGB information.) The difference between the temporal cycles of the *in situ* and MODIS LAI values may also be due to differences in the timing of phenological events of the understory and tree layer species (Richardson *et al*. 2009). Seasonal dynamics of MODIS LAI is very strong in comparison with LAI_{eff} measurements of coniferous and mixed stands (Fig. 6A and C). Thus, it seems that the spring and fall transitions of landscape-level MODIS LAI portray the phenological cycle of broadleaved species (including in a wide sense broadleaved tree layer species, understory bushes and grasses typical to open areas), not that of the coniferous tree species.

Finally, we compared the magnitude of the MODIS LAI product and the upscaled, landscape-level *in situ* LAI. At the beginning and end of the measured LAI_{eff} time series (approximate DOY 134 and 253), the MODIS LAI values were similar to the values obtained from our *in situ* measurements. However, the minimum values of MODIS LAI (i.e., DOY 97–127) were much lower than our *in situ* values obtained at the start of the growing season several weeks later. The unrealistically low MODIS LAI values do coincide with the time of spring snow melt (Fig. 1), and thus, have a plausible explanation. In July, MODIS LAI reached values as high as 4.1 whereas our *in situ* LAI_{eff} had a maximum value of 2.2 (Fig. 7).

The nearly twofold difference in maximum values also clearly indicates differences in LAI definitions between MODIS LAI and LAI_{eff} measured in this study. LAI_{eff} measured at the study sites did not account for clumping of foliage (i.e. spatial correlation of foliage at shoot and crown levels) whereas in MODIS LAI, clumping is accounted for to some extent. Compensating *in situ* LAI_{eff} for various levels of clumping would increase the LAI estimates in coniferous stands (Chen 1996). As shoot-level clumping may also change throughout the summer due to the maturation or hardening of new shoots, using a fixed value (i.e. same value for the whole growing period) to correct for it would not lead to a new interpretation of the results. Nevertheless, for the study area, the minimum MODIS LAI values are rather small considering the large coverage of coniferous forests with relatively small seasonal changes in LAI. Thus, difference in magnitude between MODIS LAI and *in situ* LAI_{eff} cannot be explained by clumping alone. This agrees well with previous MODIS LAI validation studies in evergreen coniferous sites (Yang *et al.* 2006, Garrigues *et al.* 2008). Another source of difference in the LAI definitions is that MODIS LAI includes both overstory and understory LAIs. Even though understory vegetation may fortify the seasonal dynamics of forest reflectance trajectories obtained from satellite images, it is difficult to measure LAI of a boreal forest understory plot repeatedly with non-destructive sampling methods. For example, measurement of boreal-forest understory LAI with common indirect measurement techniques (e.g. LAI-2000 Plant Canopy Analyzer or hemispherical digital photography) is not possible due to the tight structure and low height of the understory. The understory layer in a well-drained boreal forest in Finland is composed of two layers: an upper understory layer (low dwarf shrubs, graminoids, herbaceous species) and a ground layer (mosses, lichens). As bare soil is rarely visible, downward-looking hemispherical photos cannot be used to determine understory LAI_{eff}. We suggest that the noteworthy seasonality of boreal forest understory could, in the future, be included in phenological monitoring through changes in its reflectance properties (e.g. NDVI or other vegetation indices) throughout the growing season using algorithms developed for the extraction of understory reflectance from multiangular satellite data (Pisek *et al.* 2010).

Upscaling *in situ* LAI_{eff} measurements to the level of satellite vegetation products inherently contains many potential sources of error. A central question is the representativeness of sampled ground plots — how well they describe the spatial heterogeneity of the landscape, and in the case of forests, do they represent in right proportions the different age and management classes of the various forest types. For example, in this study, twenty stands cannot cover the wide range of structures present in a 7 × 7-km landscape. On the other hand, repeatedly performing optical LAI measurements (which are weather dependent) for more than twenty stands at a fairly dense temporal interval would require a large research team and exceptional sky conditions. Thus, the number of study stands under intensive LAI monitoring will always remain smaller than could be regarded as the necessary number of stands to cover all the forest types in a landscape. Using high resolution satellite images as an intermediate step to upscale to the level of MODIS products (e.g. Wang *et al.* 2004, Morisette *et al.* 2006) is a possible solution to improve landscape-level LAI estimates. However, in such an upscaling approach, it would be preferable to have a time series of high resolution satellite images, which, on the other hand, is challenging for a study site located in the boreal region due to the frequent presence of clouds.

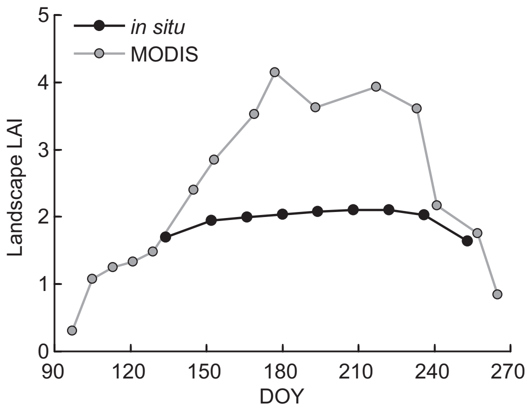

Fig. 7. Comparison of mean landscape-level LAI upscaled from *in situ* measurements and mean MODIS LAI (MOD15A2) as a function of day of year (DOY).

Conclusions

Our results showed that the timing of maximum

LAI_{eff} varies in different boreal forest types: in broadleaved and mixed stands maximal leaf area was reached by mid-July whereas in coniferous and seedling stands foliage growth marginally continued until late August. This unsynchronized timing of phenophases in fragmented and heterogeneous forest landscapes (typical to northern Europe) is a challenge for interpreting satellite observed land surface phenologies and for spatial upscaling of *in situ* LAI_{eff} time series. MODIS-based spectral vegetation indices followed the general trend of spring–summer canopy LAI well, but only RSR captured the timing of both the spring and fall transitions. The MODIS LAI product portrayed well the spring time canopy-level foliage build-up of broadleaved and seedling stands but began to decrease earlier in the fall than the field reference values. Future studies should focus on (1) understanding the driving factors of boreal forest reflectances during autumn senescence, (2) quantifying the role and timing of the phenological (reflectance) cycles of the most abundant boreal understory species, and (3) developing a better method for detecting the start and end of growing period in conifer-dominated areas.

Acknowledgements: We thank Eeva Bruun (Department of Forest Sciences, University of Helsinki) for field work, Petri Keronen (Department of Physical Sciences, University of Helsinki) for providing the meteorological data for our study site, and Pauline Stenberg and Matti Mõttus for scientific collaboration during the field campaign. This study was funded by Emil Aaltonen Foundation, University of Helsinki Research Funds, Academy of Finland, and Finnish Graduate School in Forest Sciences.

References

Brown L., Chen J.M., Leblanc S.G. & Cihlar J. 2000. A shortwave infrared modification to the simple ratio for LAI retrieval in boreal forests: an image and model analysis. *Remote Sensing of Environment* 71: 16–25.

Chen J. 1996. Optically-based methods for measuring seasonal variation of leaf area index in boreal conifer stands. *Agricultural and Forest Meteorology* 80: 135–163.

CLC2006 Finland 2006. *Finnish Corine 2006-project: final technical report*. Finnish Environment Institute, Helsinki.

Cleland E., Chuine I., Menzel A., Mooney H. & Schwartz M. 2007. Shifting plant phenology in response to global change. *Trends in Ecology and Evolution* 22: 357–365.

Eklundh L., Hall K., Eriksson H., Ardö J. & Pilesjö P. 2003. Investigating the use of Landsat thematic mapper data for estimation of forest leaf area index in southern Sweden. *Canadian Journal of Remote Sensing* 29: 349–362.

Friedl M., Henebry G., Reed B., Huete A., White M., Morisette J., Nemani R., Zhang X. & Myneni R. 2006. *Land surface phenology NASA white paper*. Available at http://landportal.gsfc.nasa.gov/Documents/ESDR/Phenology_Friedl_whitepaper.pdf.

Friedl M., Sulla-Menashe D., Tan B., Schneider A., Ramankutty N., Sibley A. & Huang X. 2010. MODIS Collection 5 global land cover: algorithm refinements and characterization of new datasets. *Remote Sensing of Environment* 114: 168–182.

Ganguly S., Friedl M., Tan B., Zhang X. & Verma M. 2010. Land surface phenology from MODIS: characterization of the Collection 5 global land cover dynamics product. *Remote Sensing of Environment* 114: 1805–1816.

Garbulsky M., Peñuelas J., Gamon J., Inoue Y. & Filella Y. 2011. The photochemical reflectance index (PRI) and the remote sensing of leaf, canopy and ecosystem radiation use efficiencies: a review and meta-analysis. *Remote Sensing of Environment* 115: 281–297.

Garrigues S., Laxaze R., Baret F., Morisette J., Weiss M., Nickeson J., Fernandes R., Plummer S., Shabanov N., Myneni R., Knyazikhin Y. & Yang W. 2008. Validation and intercomparison of global leaf area index products derived from remote sensing data. *Journal of Geophysical Research* 113, G02028, doi:10.1029/2007JG000635.

Huete A., Didan K., Miura T., Rodriguez E.P. Gao, X. & Ferreira L.G. 2002. Overview of the radiometric and biophysical performance of the MODIS vegetation indices. *Remote Sensing of Environmen*t 83: 195–213.

Jonckheere I., Fleck S., Nackaerts K., Muys B., Coppin P., Weiss M. & Baret F. 2004. Review of methods for in situ LAI determination. Part I: Theories, sensors and hemispherical photography. *Agricultural and Forest Meteorology* 121: 19–35.

Karlsen S.-R., Hogda K., Wielgolaski F., Tolvanen A., Tomervik H., Poikolainen J. & Kubin E. 2009. Growing-season trends in Fennoscandia 1986–2006 determined from satellite and phenology data. *Climate Research* 39: 275–286.

Knyazikhin Y., Martonchik J., Myneni R., Diner D. & Running S. 1998. Synergistic algorithm for estimating vegetation canopy leaf area index and fraction of absorbed photosynthetically active radiation from MODIS and MISR data. *Journal of Geophysical Research* D103: 32257–32276.

Kobayashi H., Suzuki R. & Kobayashi S. 2007. Reflectance seasonality and its relation to the canopy leaf area index in an eastern Siberian larch forest: multi-satellite data and radiative transfer analysis. *Remote Sensing of Environment* 106: 238–252.

Mathworks Inc. 2010. *MATLAB — The language of technical computing*. Available at http://www.mathworks.com/products/matlab/.

Morisette J., Privette J., Baret F., Myneni R., Nickeson J., Garrigues S., Shabanov N., Fernandes R., Leblanc S., Kalacska M., Sanchez-Azofeifa G., Chubey M., Rivard B., Stenberg P., Rautiainen M., Voipio P., Manninen T., Pilant D., Lewis T., Iiames T., Colombo R., Meroni M., Busetto L., Cohen B., Turner D., Warner E. & Petersen G. 2006. Validation of global moderate resolution LAI Products: a framework proposed within the CEOS Land Product Validation subgroup. *IEEE Transactions on Geoscience and Remote Sensing* 44: 1804–1817.

Morisette J., Richardson A., Knapp A., Fisher J., Graham E., Abatzoglou J., Wilson B., Breshears D., Hanebry G., Hanes J. & Liang L. 2009. Tracking the rhythm of the seasons in the face of global change: phenological research in the 21st century. *Frontiers in Ecology and Environment* 7: 253–260.

Nobis M. & Hunziker U. 2005. Automatic thresholding for hemispherical canopy-photographs based on edge detecting. *Agricultural and Forest Meteorology* 128: 243–250.

Pisek J., Chen J., Miller J., Freemantle J., Peltoniemi J. & Simic A. 2010. Mapping forest background in a boreal region using multiangle Compact Airborne Spectrographic Imager data. *IEEE Transactions on Geoscience and Remote Sensing* 48: 499–510.

Rautiainen M., Nilson T. & Lükk T. 2009. Seasonal reflectance trends of hemiboreal birch forests. *Remote Sensing of Environment* 113: 805–815.

Rautiainen M. & Stenberg P. 2005. Application of photon recollision probability in simulating coniferous canopy reflectance. *Remote Sensing of Environment* 96: 98–107.

Richardson A., Jenkins J., Braswell B., Hollinger D., Ollinger S. & Smith M.-L. 2007. Use of digital webcam images to track spring green-up in a deciduous broadleaf forest. *Oecologia* 152: 323–334.

Richardson A. & O'Keefe J. 2009. Phenological differences between understory and overstory: a case study using the long-term Harvard Forest records. In: Noormets A. (ed.), *Phenology of ecosystem processes*, Springer Science + Business Media, pp. 87–117.

Vermote E.F., El Saleous N.Z., Justice C.O., Kaufman Y.J., Privette J., Remer L., Roger J.C. & Tanré D. 1997. Atmospheric correction of visible to middle infrared EOS-MODIS data over land surface, background, operational algorithm and validation. *Journal of Geophysical Research* 102(D14): 17131–17141.

Wang Y., Woodcock C.E., Buermann W., Stenberg P., Voipio P., Smolander H., Häme T., Tian Y., Hu J., Knyazikhin Y. & Myneni R.B. 2004. Evaluation of the MODIS LAI algorithm at a coniferous forest site in Finland. *Remote Sensing of Environment* 91: 114–127.

Welles J. & Norman J. 1991. Instrument for indirect measurement of canopy architecture. *Agronomy Journal* 83: 818–825.

White M., Beurs K., Didan K., Inouyes D., Richardson A., Jensen O., O'Keefe J., Zhnag G., Nemani R., van Leeweun W., Brown J., Wit A., Schaepman M., Lin X., Dettinger M., Bailey A., Kimball J., Schwartz M., Baldocchi D., Lee J. & Lauenroth W. 2009. Intercomparison, interpretation, and assessment of spring phenology in North America estimated from remote sensing for 1986–2006. *Global Change Biology* 15: 2335–2359.

Yang W., Shabanov N., Huang D., Wang W., Dickinson R., Nemani R., Knyazikhin Y. & Myneni R. 2006. Analysis of leaf area index products from combination of MODIS Terra and Aqua data. *Remote Sensing of Environment* 104: 297–312.

Zhang Y., Chen J.M. & Miller J.R. 2005. Determining digital hemispherical photograph exposure for leaf area index estimation. *Agricultural and Forest Meteorology* 133: 166–181.

Zhang X., Friedl M., Schaaf C., Strahler A., Hodges J., Gao F., Reed B. & Huete A. 2003. Monitoring vegetation phenology using MODIS. *Remote Sensing of Environment* 84: 471–475.